Science Advances
AAAS

advances.sciencemag.org/cgi/content/full/6/14/eaay2801/DC1

Supplementary Materials for

A chemically unmodified agonistic DNA with growth factor functionality for in vivo therapeutic application

Ryosuke Ueki*, Satoshi Uchida, Naoto Kanda, Naoki Yamada, Ayaka Ueki, Momoko Akiyama, Kazuko Toh, Horacio Cabral, Shinsuke Sando*

*Corresponding author. Email: r.ueki@chembio.t.u-tokyo.ac.jp (R.U.); ssando@chembio.t.u-tokyo.ac.jp (S.S.)

Published 1 April 2020, *Sci. Adv.* **6**, eaay2801 (2020)
DOI: 10.1126/sciadv.aay2801

The PDF file includes:

Other Supplementary Material for this manuscript includes the following:

(available at advances.sciencemag.org/cgi/content/full/6/14/eaay2801/DC1)

Supplementary materials

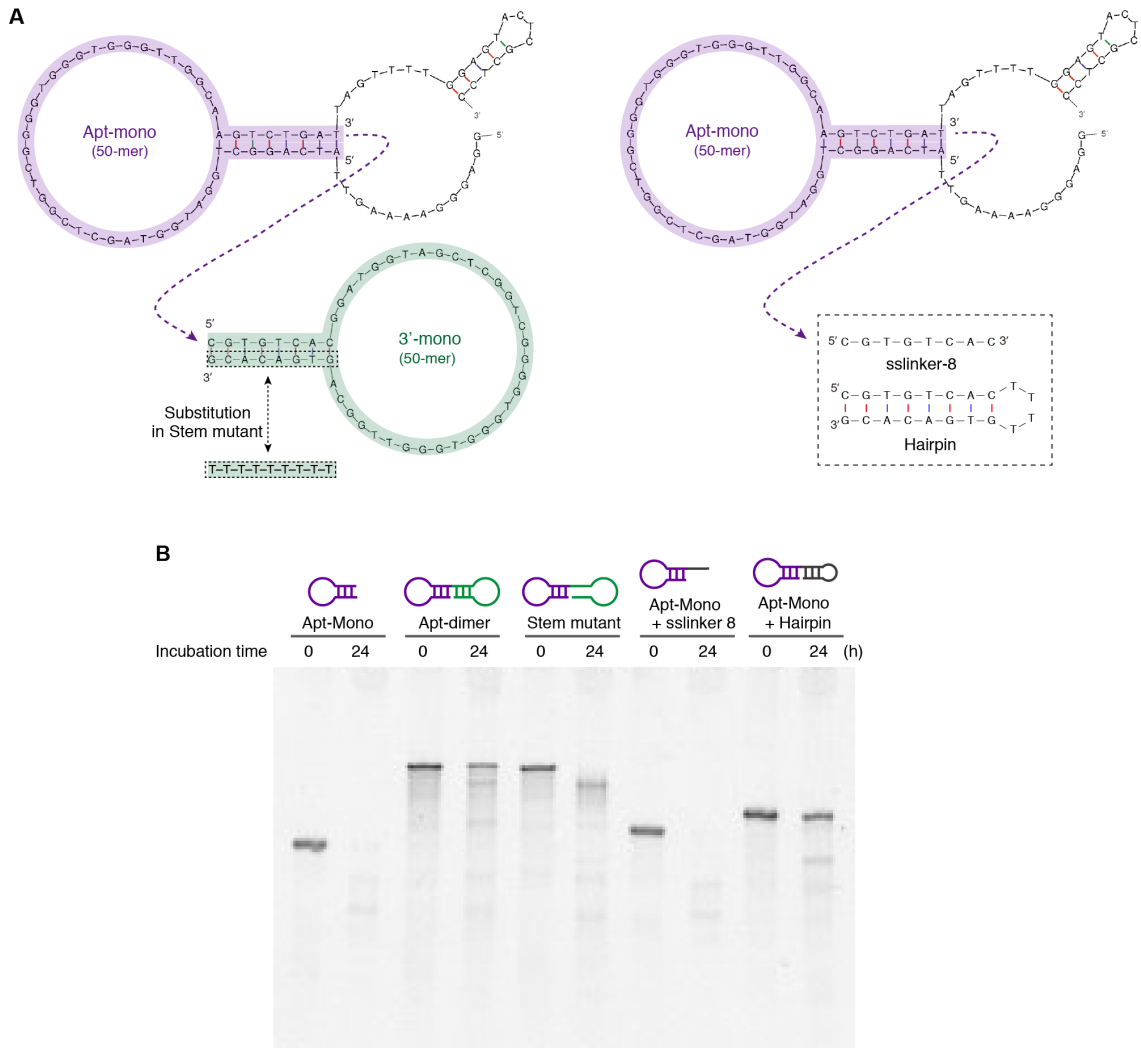

Fig. S1 Nuclease stability of the Apt-dimer and its mutants. (**A**) Schematic representation of sequence of the Apt-dimer and its mutants. The sequence of "sslinker-8" is derived from the 5′-terminal sequence of 3′-mono. The stem sequence of "Hairpin" is derived from that of 3′-mono, while its loop sequence was replaced with $(dT)_4$ sequence. (**B**) Nuclease stability of the oligonucleotides. Each oligonucleotide (2 μM) was incubated in phosphate-buffered saline containing 50% fetal bovine serum at 37 °C. After incubation, the samples were immediately analysed with denaturing 15% polyacrylamide gel electrophoresis.

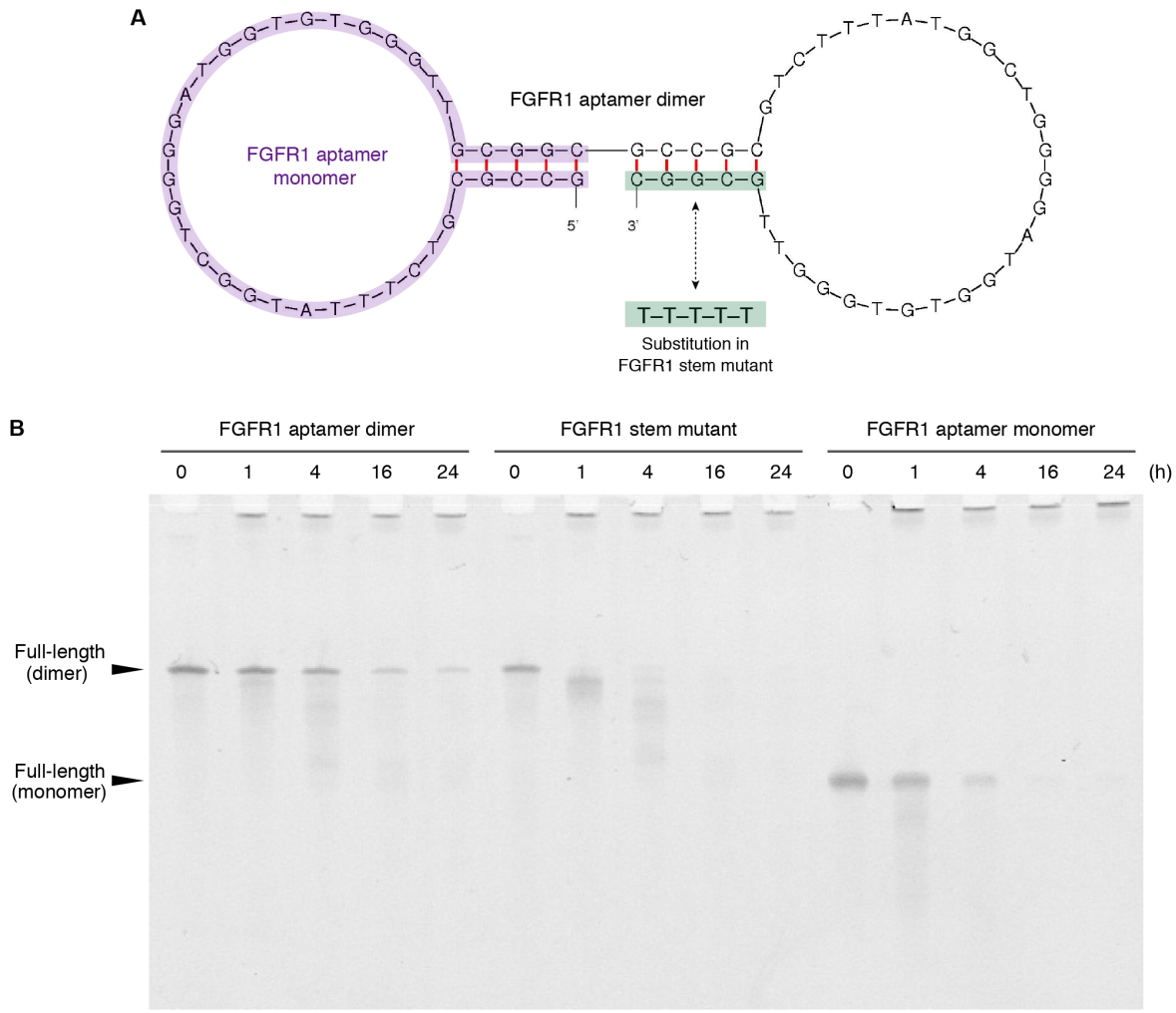

Fig. S2 Nuclease stability of FGFR-binding aptamer and its mutants. (**A**) A predicted secondary structure of an agonistic FGFR1 aptamer (FGFR1 aptamer dimer, named as "TD0" in the original paper) that was calculated using Mfold. The monomeric aptamer sequence (FGFR1 aptamer monomer, named as "SL38.2" in the original paper) and poly-T substitution introduced to "FGFR1 stem mutant" are highlighted in purple and green, respectively. (**B**) Nuclease stability of the oligonucleotides. Each oligonucleotide (2 μM) was incubated in phosphate-buffered saline containing 50% fetal bovine serum at 37 °C. After incubation, the samples were immediately analysed with denaturing 15% polyacrylamide gel electrophoresis.

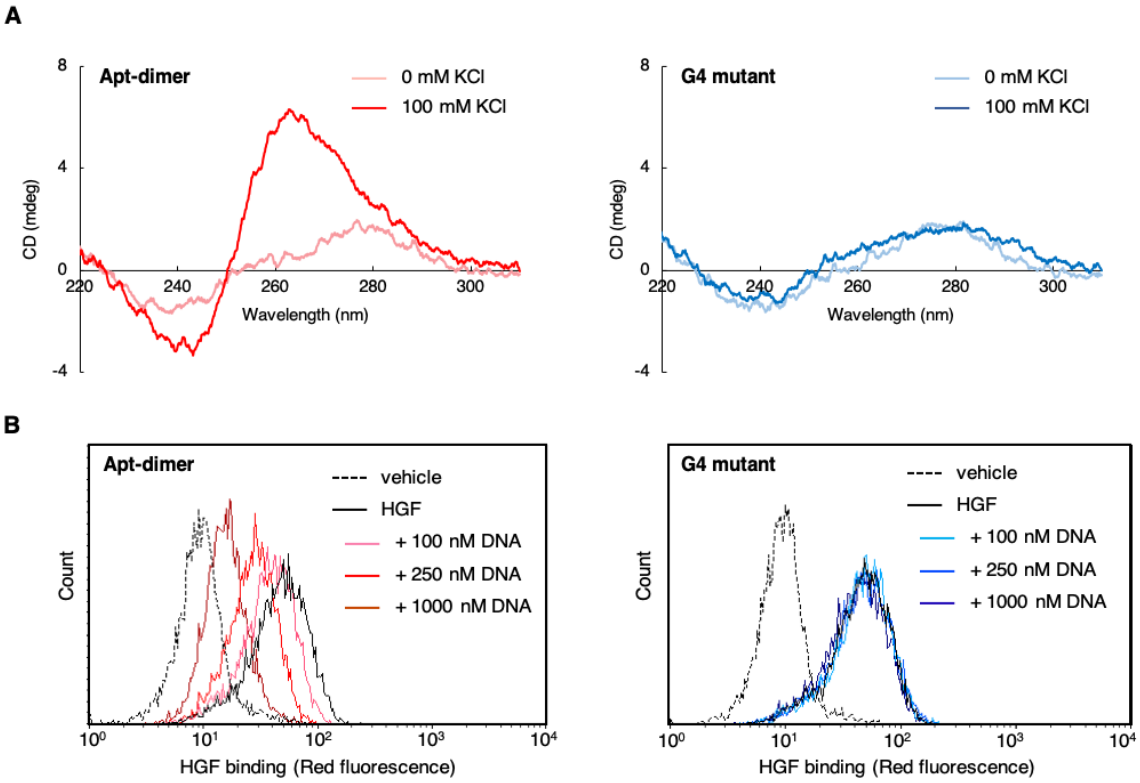

Fig. S3 CD spectra and flow cytometric analysis of the Apt-dimer and G4 mutant. (A) CD spectra of the Apt-dimer (left, 2.5 μM) and G4 mutant (right, 2.5 μM) in 20 mM Tris–HCl buffer (pH 7.6) supplemented with KCl (0 or 100 mM) at 37 ˚C. **(B)** Competition assay of HGF binding to the Met-expressing SNU-5 cells in the presence of either Apt-dimer or G4 mutant. The SNU-5 cells were incubated with Hilyte Fluor 647 labelled-HGF (5 nM) and aptamer (100–1000 nM) for 15 min at 37 ˚C.

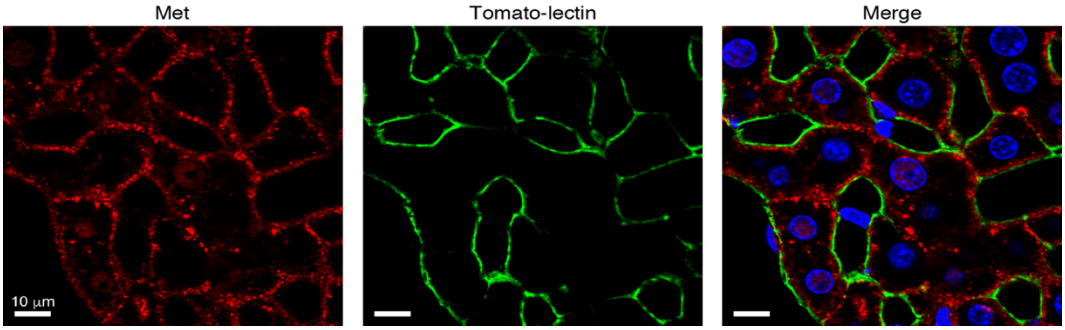

Fig. S4 Immunohistochemical analysis of Met in liver tissues. The liver sections were excised from non-treated mice and then stained with anti-Met antibody (red). The endothelial cells and nuclei were stained with DyLight 488-labeled tomato lectin (green) and Hoechst 33342 (blue), respectively. The sections were observed using a confocal laser-scanning microscope. The signals from Met and Tomato-lectin showed almost no detectable colocalization, indicating that Met expresses mainly in liver parenchyma, and minimally in endothelial cells. Scale bar: 10 μm.

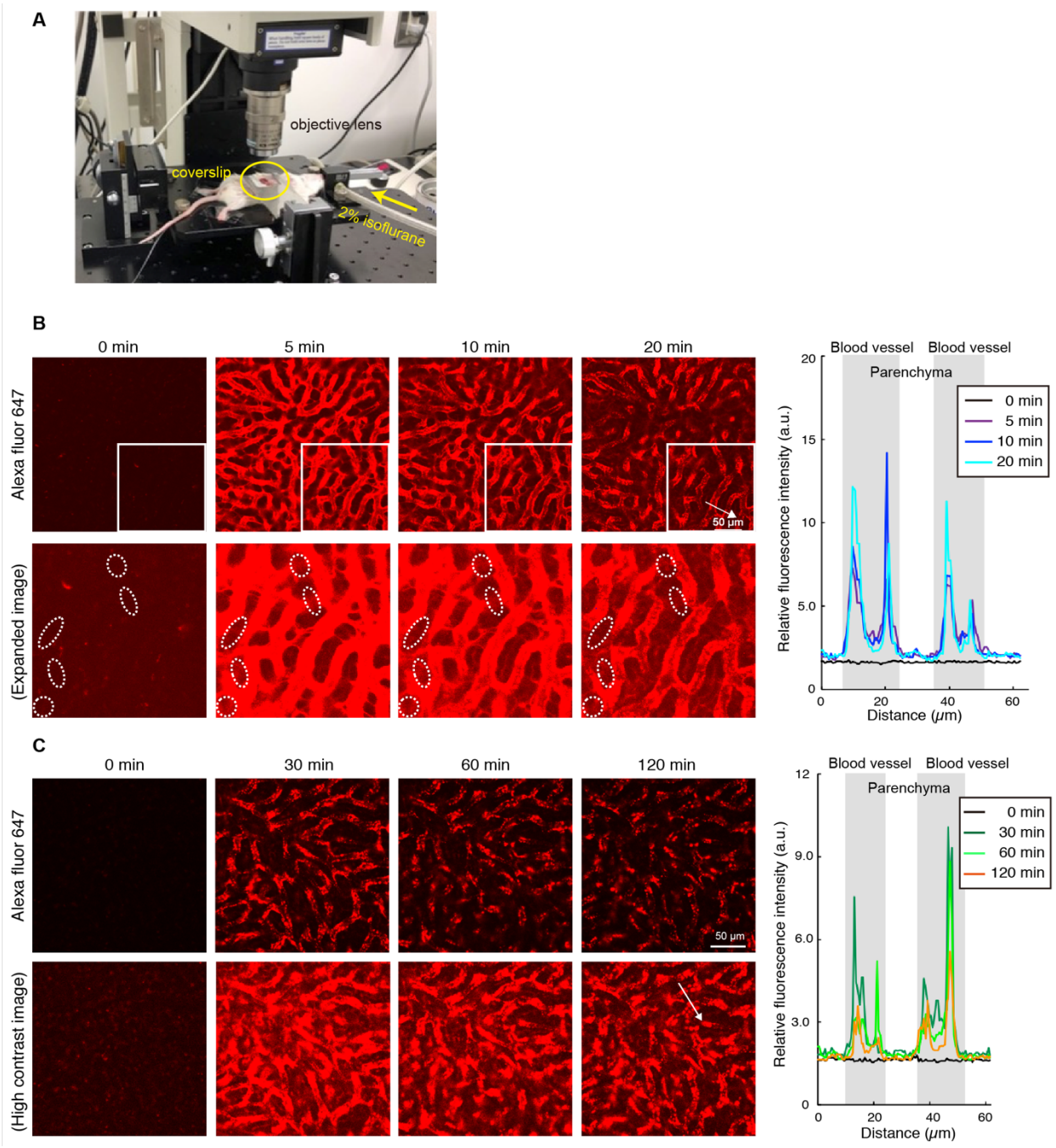

Fig. S5 Intravital imaging of the Apt-dimer in the liver. (**A**) Observation setup of IVRTCLSM imaging. (**B**) Intravital imaging of the Apt-dimer (5′-Alexa Fluor 647) in the liver. The same experiment as that of Fig. 3A was performed using a mouse different from that used the experiment. Lower figures show enlarged and brighter images of square region in upper figures. Dotted circles highlight the leakage of Apt-dimer to liver parenchyma. The right panel shows the intensity profile of Alexa Fluor 647 in the region indicated with the white arrows in the left panel. (**C**) Long-term intravital imaging of the Apt-dimer (5′-Alexa Fluor 647) in the liver. Lower figures show brighter images of the upper figures. The right panel shows the intensity profile of Alexa Fluor 647 in the region indicated with the white arrows in the left panel.

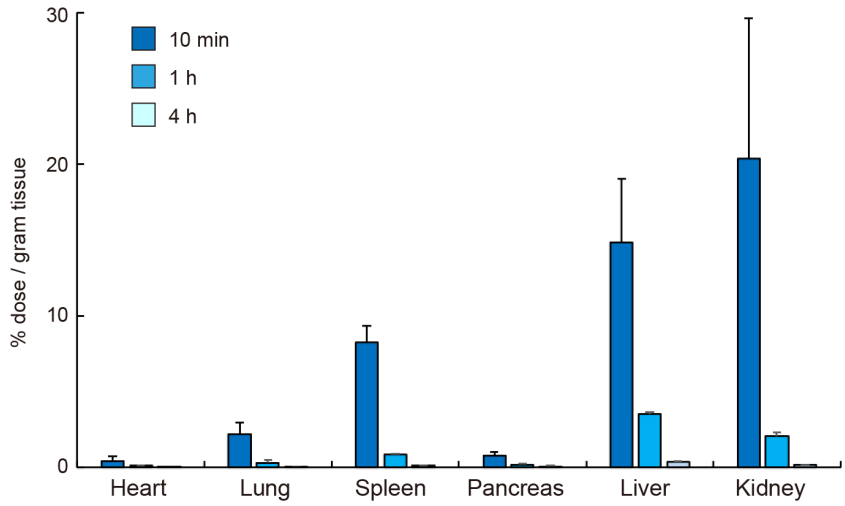

Fig. S6 Tissue distribution of the Apt-dimer. Tissue distribution of the 5′-Alexa Fluor-647-labelled Apt-dimer after the indicated time from the systemic injection. The amount of DNA was quantified by fluorescence intensity in the supernatant of the organ homogenates. The results are expressed as the mean ± SD (n = 3).

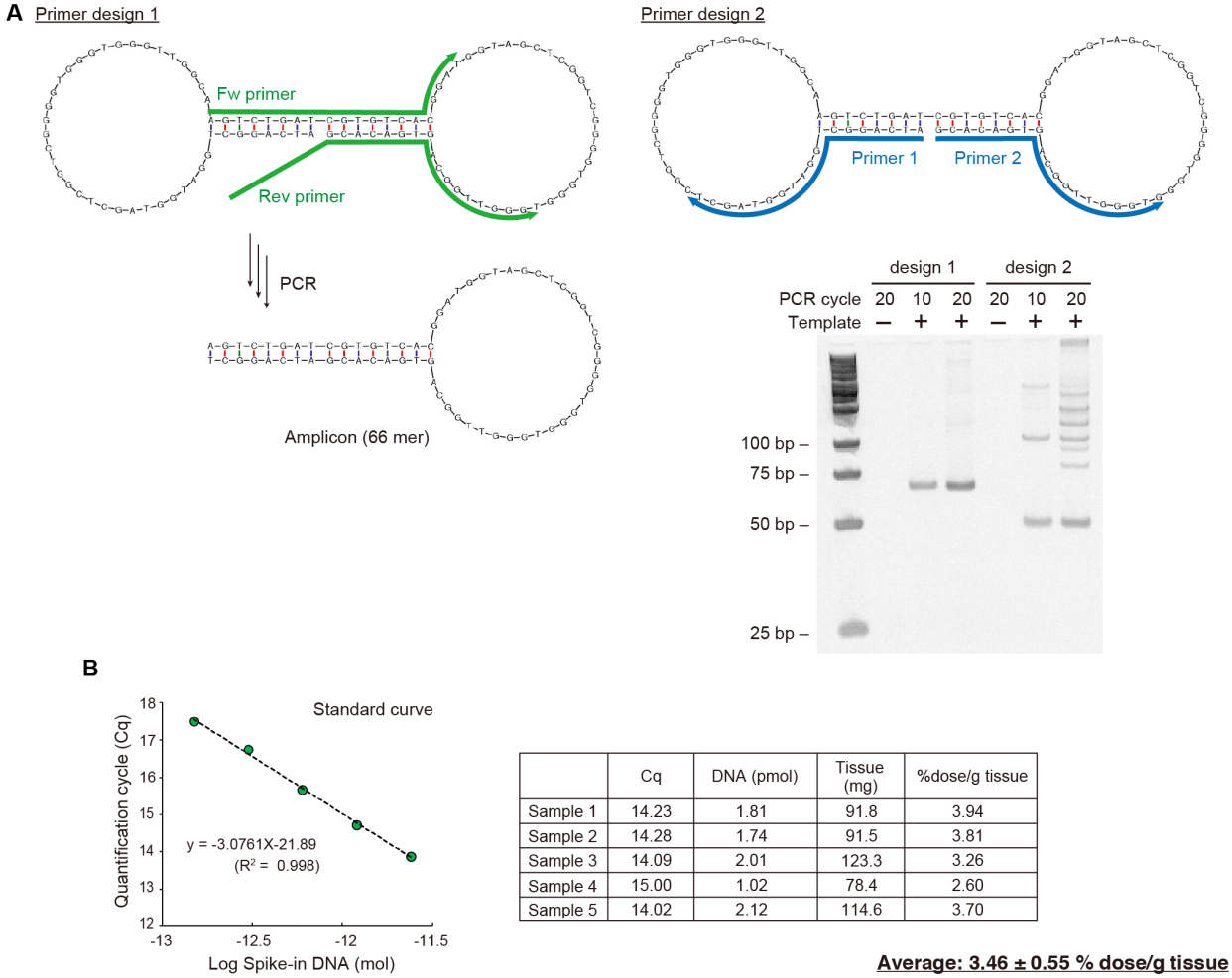

	Cq	DNA (pmol)	Tissue (mg)	%dose/g tissue
Sample 1	14.23	1.81	91.8	3.94
Sample 2	14.28	1.74	91.5	3.81
Sample 3	14.09	2.01	123.3	3.26
Sample 4	15.00	1.02	78.4	2.60
Sample 5	14.02	2.12	114.6	3.70

Average: 3.46 ± 0.55 % dose/g tissue

Fig. S7 Quantitative PCR analysis of the Apt-dimer distributed to liver. (A) Schematic presentation of primer design for the detection of Apt-dimer. Primer design 1 produced single amplicon after PCR cycles, while Primer design 2 produced several amplicons. (B) Quantitative PCR analysis of Apt-dimer distributed to liver after 10 min from systemic injection (10 nmol). The set of primer shown in "Primer design 1" in Fig. S6A was used for PCR amplification. The standard curve was obtained by using aptamer-spike in liver homogenate samples.

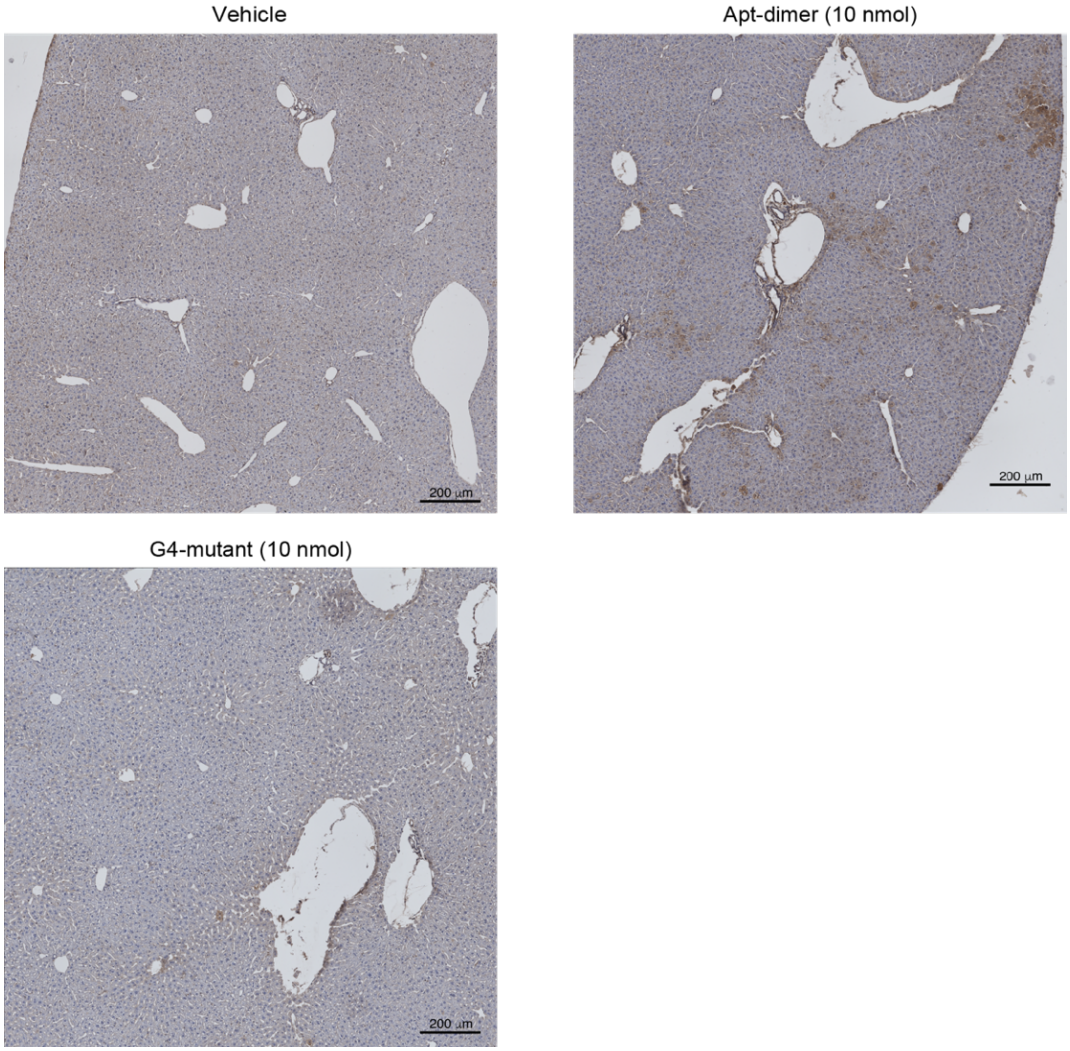

Fig. S8 Immunohistochemistry of Met activation in the mouse liver after intravenous injection of the oligonucleotides. Low magnification images of immunohistochemistry analysis of Met phosphorylation in mouse liver. Scale bars indicate 200 μm.

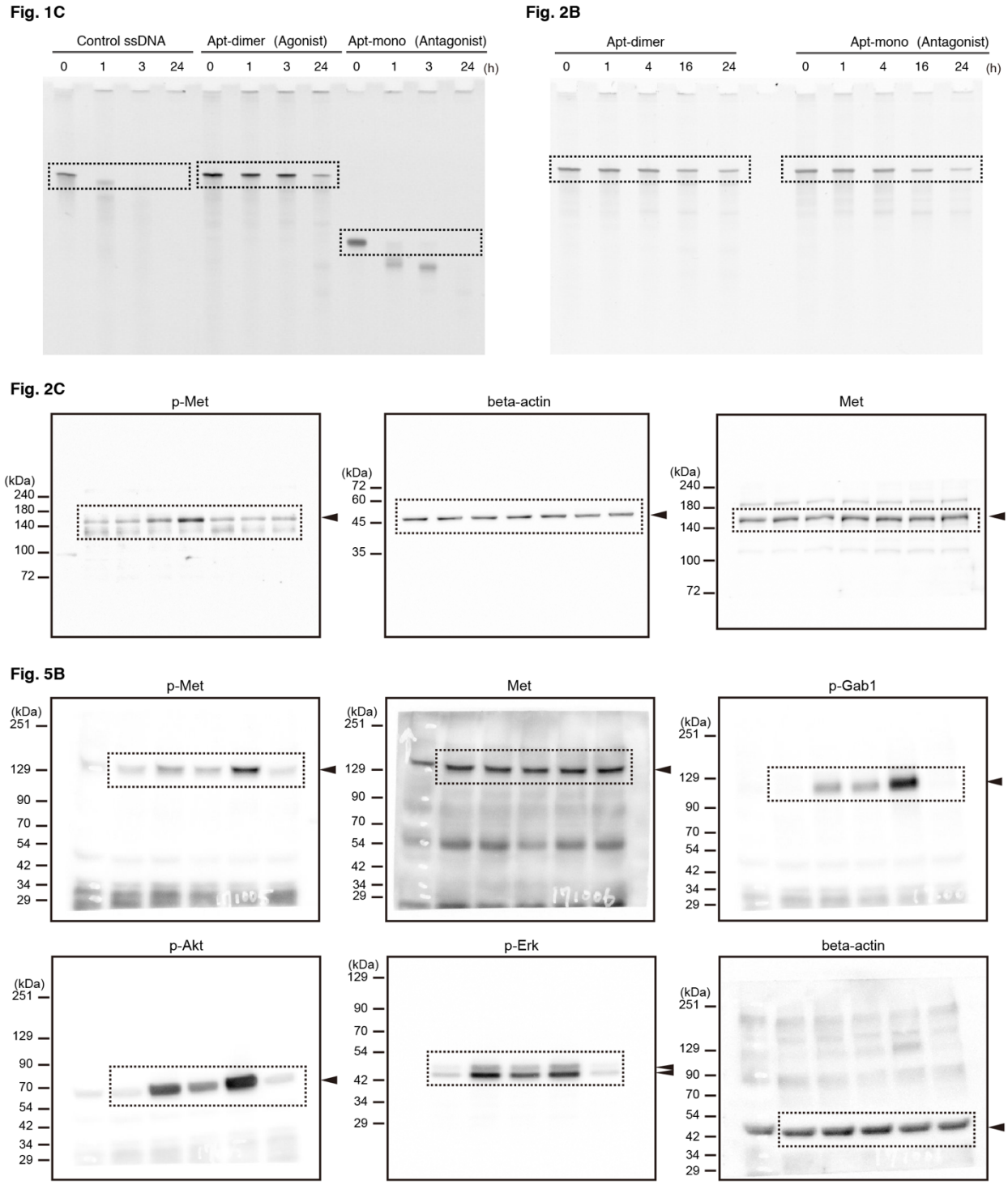

Fig. S9 Uncropped images of denaturing PAGE and Western blotting.

Table S1 Sequence data.

Name of sequence	Sequence
Apt-dimer	ATC AGG CTG GAT GGT AGC TCG GTC GGG GTG GGT GGG TTG GCA AGT CTG ATC GTG TCA CGG ATG GTA GCT CGG TCG GGG TGG GTG GGT TGG CAG TGA CAC G
Apt-mono	ATC AGG CTG GAT GGT AGC TCG GTC GGG GTG GGT GGG TTG GCA AGT CTG AT
3'-mono	CGT GTC ACG GAT GGT AGC TCG GTC GGG GTG GGT GGG TTG GCA GTG ACA CG
Control ssDNA	TCA ATC CAT CAT TTA CTC ATG CTA ACA CCA ACT ATT TGC CTT CTA CTA ACG AAC TCT TTG TGC CTA CCA TCC TCA TAC TTA CTA GAA CGA TAA CAC TAT C
G4 mutant	ATC AGG CTG GAT GAT AGC TCG GTC GGG GTG GAT GGG TTG GCA AGT CTG ATC GTG TCA CGG ATG ATA GCT CGG TCG GGG TGG ATG GGT TGG CAG TGA CAC G
Stem mutant	ATC AGG CTG GAT GGT AGC TCG GTC GGG GTG GGT GGG TTG GCA AGT CTG ATC GTG TCA CGG ATG GTA GCT CGG TCG GGG TGG GTG GGT TGG CAT TTT TTT T
Apt-mono + sslinker-8	ATC AGG CTG GAT GGT AGC TCG GTC GGG GTG GGT GGG TTG GCA AGT CTG ATC GTG TCA C
Apt-mono + hairpin	ATC AGG CTG GAT GGT AGC TCG GTC GGG GTG GGT GGG TTG GCA AGT CTG ATC GTG TCA CTT TTG TGA CAC G
FGFR1 aptamer dimer	GCC GCG TCT TTA TGG CTG GGG ATG GTG TGG GTT GCG GCG CCG CGT CTT TAT GGC TGG GGA TGG TGT GGG TTG CGG C
FGFR1 stem mutant	GCC GCG TCT TTA TGG CTG GGG ATG GTG TGG GTT GCG GCG CCG CGT CTT TAT GGC TGG GGA TGG TGT GGG TTT TTT T
FGFR1 aptamer monomer	GCC GCG TCT TTA TGG CTG GGG ATG GTG TGG GTT GCG GC
Fw primer	AGT CTG ATC GTG TCA CGG AT
Rev primer	AGC CTG ATC GTG TCA CTG CCA ACC CA

Movies S1 to S4

Movie S1. Intravital real-time imaging of liver tissues after systemic injection of the 5′-Alexa Fluor 647-labelled Apt-dimer (Fig. 3A).

Movie S2. Intravital real-time imaging of liver tissues after systemic injection of the 5′-Alexa Fluor 647-labelled G4 mutant (Fig. 3B).

Movie S3. Intravital real-time imaging of liver tissues after systemic injection of Alexa Fluor 647 (Fig. 3C).

Movie S4. Intravital real-time imaging of liver tissues after systemic injection of the 5′-Alexa Fluor 647-labelled Apt-dimer (Fig. S5C).

Additional supplementary file

Table. 1

	after 24 h		after 7 d	
	vehicle (N = 4)	Apt-dimer (N = 4)	vehicle (N = 4)	Apt-dimer (N = 5)
AST (IU/L)	51.5 ± 8.3	40.0 ± 5.2	47.0 ± 4.2	43.0 ± 1.6
ALT (IU/L)	34.5 ± 8.4	25.5 ± 6.0	31.8 ± 5.3	23.4 ± 1.1
BUN (mg/dL)	20.8 ± 3.1	19.3 ± 3.2	21.8 ± 4.0	21.8 ± 5.1
Cre (mg/dL)	0.09 ± 0.01	0.09 ± 0.01	0.09 ± 0.02	0.09 ± 0.01
LDH (IU/L)	413 ± 173	238 ± 67	401 ± 40	425 ± 133
T-Bil (mg/dL)	0.06 ± 0.01	0.04 ± 0.01	0.04 ± 0.01	0.05 ± 0.02
Amy (IU/L)	2676 ± 830	1973 ± 269	2425 ± 444	2271 ± 582
Na (mEq/L)	148.5 ± 1.9	149.3 ± 1.5	148.3 ± 1.0	148.4 ± 1.3
K (mEq/L)	3.2 ± 0.2	3.6 ± 0.4	3.1 ± 0.2	3.7 ± 0.9
Cl (mEq/L)	107.8 ± 1.7	110.0 ± 1.4	108.3 ± 1.7	108.8 ± 1.1

Table 1. Blood tests 24 h and 7 d after administering the single intravenous injection of the vehicle control (DPBS) or Apt-dimer (10 nmol). The results are expressed as the Mean ± SD.

Fig. 1

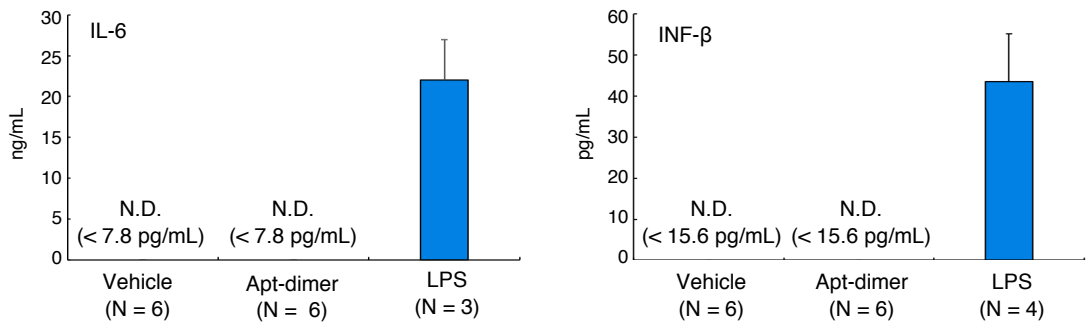

Fig. 1 Serum levels of pro-inflammatory molecules. Concentrations of interleukin 6 (IL-6) and interferon β (IFN-β) were measured 4 h after the injecting the vehicle control (DPBS) or Apt-dimer (10 nmol). Serum samples prepared after 1.5 h (for INF-β detection) or 4 h (for IL-6 detection) from the intraperitoneal injection of lipopolysaccharide (LPS) were used as the positive controls. N.D.: not-detected.

Fig. 2

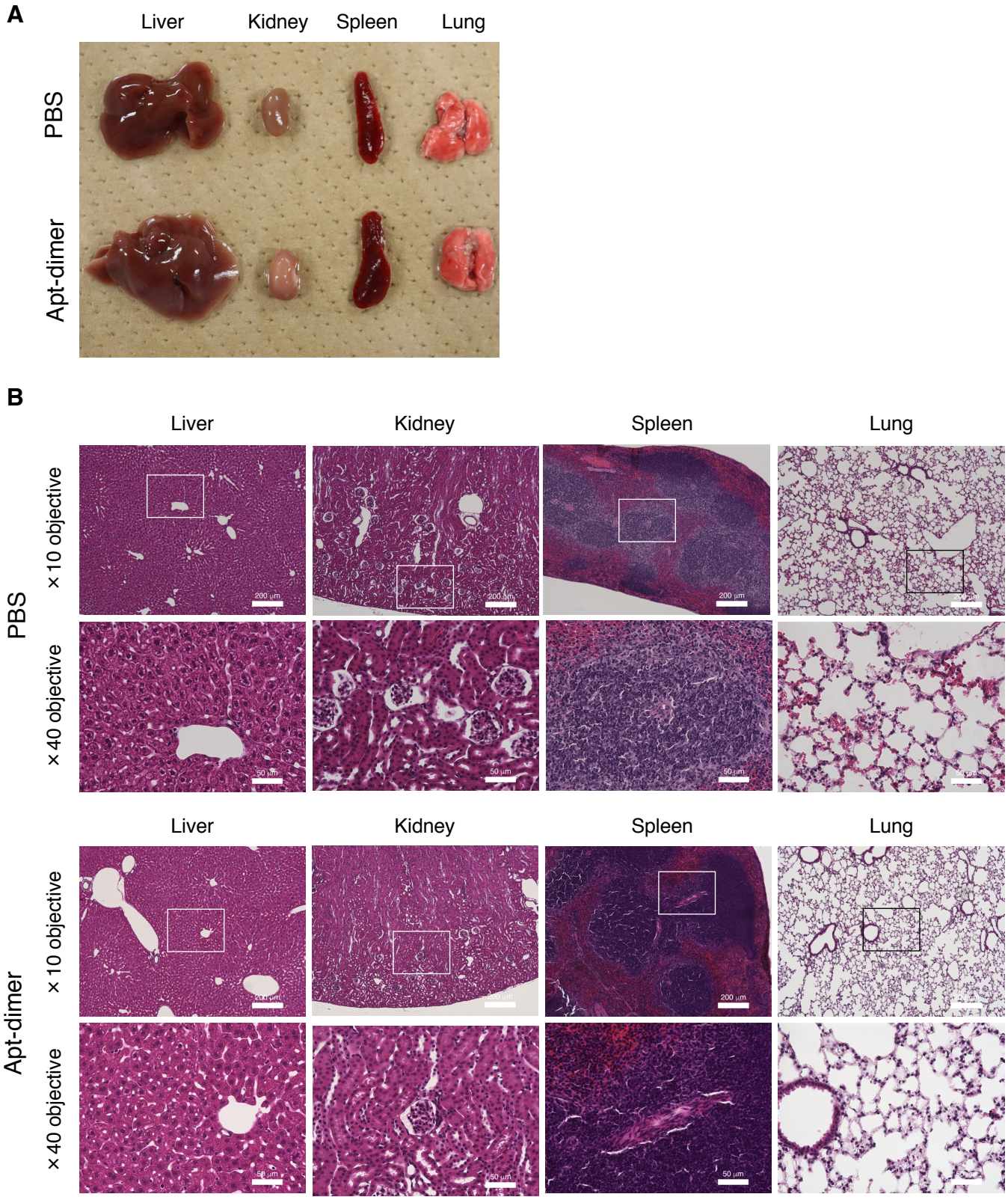

Fig. 2 (A) Gross morphology images, and (B) Representative images of H&E staining of tissues after 24 h from the administration of single intravenous injection of the vehicle (PBS) or Apt-dimer (10 nmol).

Fig. 3

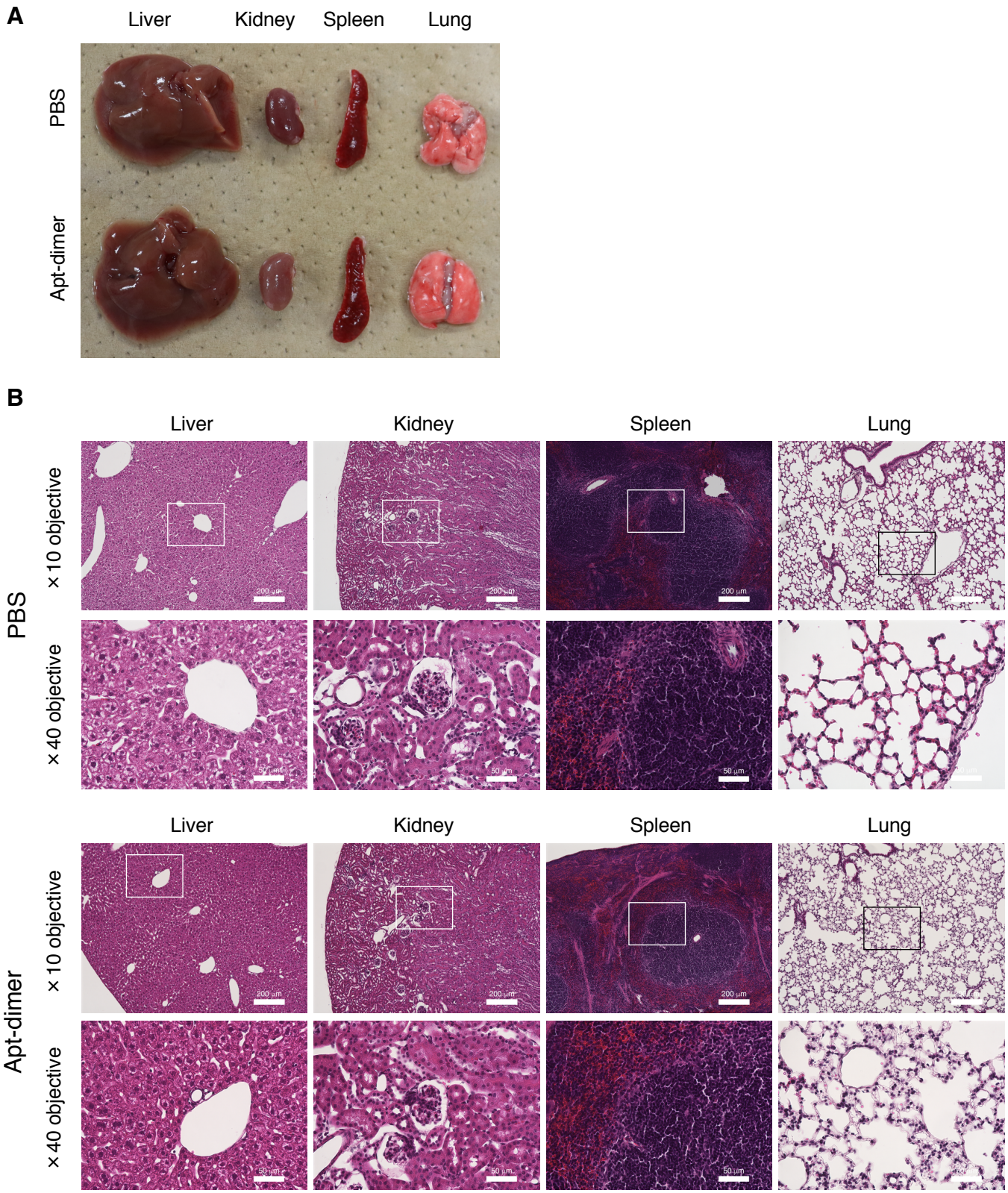

Fig. 3 (A) Gross morphology images, and (B) Representative images of H&E staining of tissues after 7 d from the administration of single intravenous injection of the vehicle (PBS) or Apt-dimer (10 nmol).